

## Counter rotating type hydroelectric unit suitable for tidal power station

To cite this article: T Kanemoto and T Suzuki 2010 *IOP Conf. Ser.: Earth Environ. Sci.* **12** 012111

View the [article online](#) for updates and enhancements.

### Related content

- [Counter-rotating type axial flow pump unit in turbine mode for micro grid system](#)  
R Kasahara, G Takano, T Murakami et al.
- [Operation of the counter-rotating type pump-turbine unit installed in the power stabilizing system](#)  
T Kanemoto, H Honda, R Kasahara et al.
- [Effect of inner guide on performances of cross flow turbine](#)  
K Kokubu, K Yamasaki, H Honda et al.

### Recent citations

- [Experimental investigation into the effects of blade pitch angle and axial distance on the performance of a counter-rotating tidal turbine](#)  
Xuesong Wei *et al*



**IOP | ebooks™**

Bringing you innovative digital publishing with leading voices to create your essential collection of books in STEM research.

Start exploring the collection - download the first chapter of every title for free.

# Counter rotating type hydroelectric unit suitable for tidal power station

T Kanemoto<sup>1</sup> and T Suzuki<sup>2</sup>

<sup>1</sup>Faculty of Engineering, Kyushu Institute of Technology, Sensui 1-1, Tobata, Kitakyushu 804-8550, Japan

<sup>2</sup>Graduate School of Engineering, Kyushu Institute of Technology, Sensui 1-1, Tobata, Kitakyushu 804-8550, Japan

E-mail: turbo@tobata.isc.kyutech.ac.jp

**Abstract.** The counter rotating type hydroelectric unit, which is composed of the axial flow type tandem runners and the peculiar generator with double rotational armatures, was proposed to utilize effectively the tidal power. In the unit, the front and the rear runners counter drive the inner and the outer armatures of the generator, respectively. Besides, the flow direction at the rear runner outlet must coincide with the flow direction at the front runner inlet, because the angular momentum through the rear runner must coincide with that through the front runner. That is, the flow runs in the axial direction at the rear runner outlet while the axial inflow at the front runner inlet. Such operations are suitable for working at the seashore with rising and falling tidal flows, and the unit may be able to take place of the traditional bulb type turbines. The tandem runners were operated at the on-cam conditions, in keeping the induced frequency constant. The output and the hydraulic efficiency are affected by the adjustment of the front and the blade setting angles. The both optimum angles giving the maximum output and/or efficiency were presented at the various discharges/heads. To promote more the tidal power generation by this type unit, the runners were also modified so as to be suitable for both rising and falling flows. The hydraulic performances are acceptable while the output is determined mainly by the trailing edge profiles of the runner blades.

## 1. Introduction

To cope with the warming global environments, the hydropower should occupy the attractive attention of the electric power generation systems as clean and sustainable energy source with highest density, in cooperation with the wind and the solar powers. That is, we should make effort to utilize effectively the large/small/mini/micro hydropower not only on the land but also on the ocean, without nature disruptions. For contributing fruitfully to such demands, it is required to prepare more several types of the hydroelectric unit suitable for the individual hydro-circumstances.

The propeller type, Darrieus type and the cross-flow type hydraulic turbines have been prepared for the small hydropower on the land and/or the ocean (e.g. <http://www> [1], Furukawa et al. [2], Fukutomi and Nakase [3]). The unique turbine with the counter-rotating runners has been proposed (Nielsen et al. [4]), and the author also invented the counter-rotating type hydroelectric unit, which is composed of the tandem runners and the peculiar generator with the double rotational armatures (Kanemoto et al. [5]). In this unit, the front and the rear runners counter-drive the inner and the outer armatures of the peculiar generator, respectively, while the rotational torque is counter-balanced successfully in the runners/armatures. The unit has promising advantages that not only the output voltage is sufficiently high without supplementary equipments such as a gearbox, but also the rotational moment hardly acts on the mounting bed owing to the momentum balance. That is, it is not necessary to set rigidly the unit on the mounting bed anchored to the ground. The fundamental performances and the flow conditions around the runners have been investigated and the design data for the runners have been presented (Tanaka et al. [6]).

This type hydroelectric unit can be supplied to not only the hydropower on the land but also the tidal power

on the ocean, in place of the traditional bulb type turbines. In this paper, this unit is operated at the on-cam condition in response to the gradual change of the tidal head at the power station. At the tidal power station with the traditional type hydroelectric unit, a pair of the units, whose inlet and outlet are replaced each other, must be set uselessly in general, to get the fruitful output from not only the rising but also the falling tides at the station with the dam/weir/sluiice. Then, the runner blades are modified so as to work effectively at the bidirectional flows, and the hydraulic performances are also investigated experimentally and numerically.

## 2. Counter-Rotating Type Hydroelectric Unit

### 2.1 Model Unit

The model counter-rotating type hydroelectric unit is shown in Fig. 1 and the velocity triangles around the axial flow type runner blade are shown in Fig. 2. The axial flow at the inlet section gives the rotational torque to the front runner, and swirls at the outlet section. Its swirling flow gives again the counter-rotational torque to the rear runner, and runs into the axial direction. It means that the angular momentum change through the front runner must coincide with the angular momentum change through the rear runner, while the rotational torque is counter-balance between the inner and the outer armatures. Then, the runners successfully counter-drive the inner and the outer armatures of the generator, respectively.

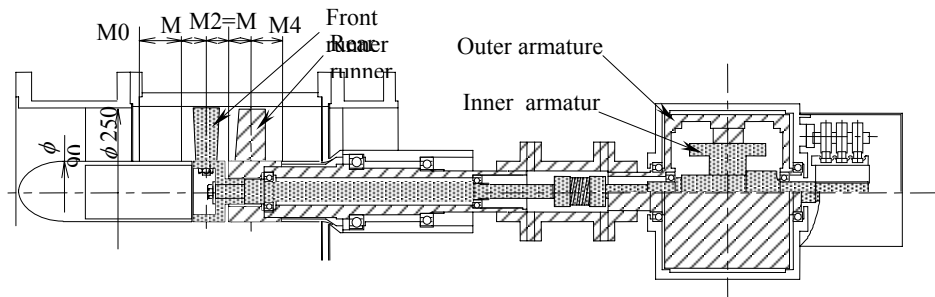


Fig. 1 Model counter-rotating type hydroelectric unit

### 2.2 Synchronous Generator

Taking account of supplying the output not only to the grid but also to the isolated power systems, the model counter-rotating armature type synchronous generator with the inner and the outer rotational armatures (3-phases, 4-poles, permanent magnet, AC generator with the double rotational armatures) shown in Fig. 3, was prepared. The rated output  $P$  is 1 kW at the relative rotational speed  $N_T = 1500 \text{ min}^{-1}$ , while the induced frequency is  $f = 50 \text{ Hz}$  and the induced voltage is  $E = 100\text{V}$ . The characteristics were investigated experimentally, where the armatures were driven by two motors, respectively, in place of the proposed tandem runners.

Figure 4 shows the relation of the rotational torque between the inner armature  $T_F^*$  and the outer armature  $T_R^*$ , in keeping the rotational speed of the inner armature constant at  $N_F = 750 \text{ min}^{-1}$ , while the rotational speed of the outer armature  $N_R$  was changed variously by the external loads. These values  $T_F^*$ ,  $T_R^*$  do not have the mechanical torques of the bearings and the slip ring to know the fundamental characteristics, and  $T_R^*$  is given by the absolute value though  $T_R^*$  is in the opposite direction to  $T_F^*$ . It is obviously confirmed that  $T_R^*$  coincides strictly with  $T_F^*$  irrespective of the relative rotational speed  $N_T (= N_F - N_R)$  and the output/load, because the rotational torques should be counter-balanced dynamically between the inner and the outer armatures.

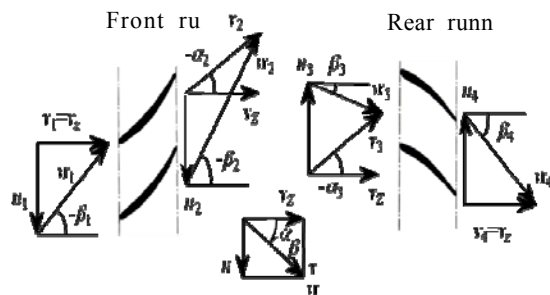


Fig. 2 Velocity triangles through the counter-

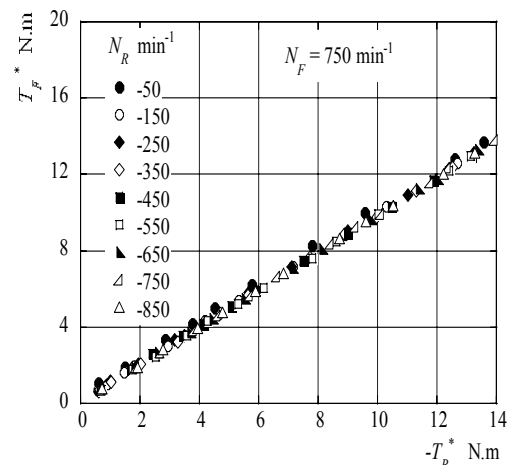
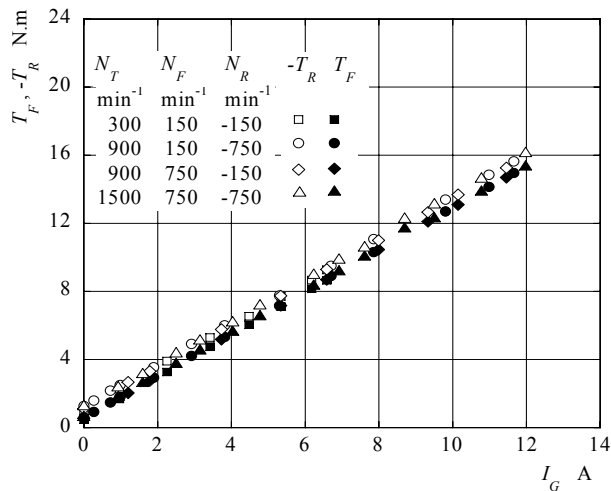


Fig. 4 Rotational torque between the inner and



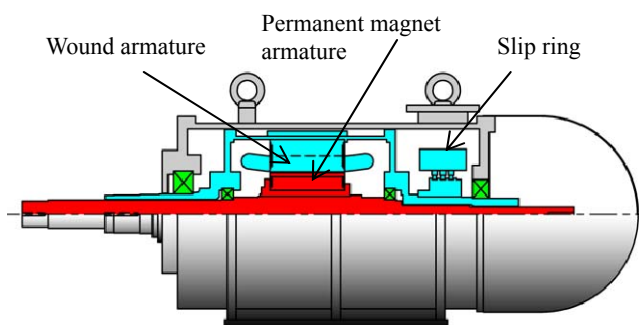
**Fig. 5** Rotational torques against the induced electric current

Figure 5 shows the rotational torques  $T_F$  and  $T_R$  (absolute value) against the induced electric current  $I_G$ , at the various relative speeds  $N_T$ , where these torques include the mechanical torques to know the characteristics in the practical use. The torques  $T_F$ ,  $T_R$  are in proportion to the induced electric current  $I_G$ , but the torque  $T_R$  of the outer armature is slightly larger than  $T_F$  of the inner armature due to the mechanical torque of the larger bearings and slip ring.

The output  $P$  and the induced voltage  $E$  against the induced electric current  $I_G$  are determined by the relative rotational speed  $N_T (= N_F - N_R)$ , as shown in Fig. 6. The output increases with the increase of the voltage  $E$  at the same  $I_G$  and increases with the increase of  $I_G$  at the same  $N_T$ , while  $E$  is proportional to  $N_T$ .

### 2.3 Doubly Fed Induction Generator

The doubly fed induction generator is boarded on the power unit with large capacity for making the output supply to the grid system (Muller et al. [7]). It is not necessary to control mechanically the runner speeds for guaranteeing precisely the induce frequency for the grid system. The frequency  $f_1$  induced from the outer armature (the primary feed) can be easily kept constant by modulating the frequency  $f_2$  of the inverter connected to the inner armature (the secondary feed) in response to the relative runner speed. The output  $P_1$  and the voltage  $E_1$  induced from the outer armature can also be kept constant, by modulating the input  $P_2$  and the voltage  $E_2$



**Fig. 3** Model double rotational type synchronous generator

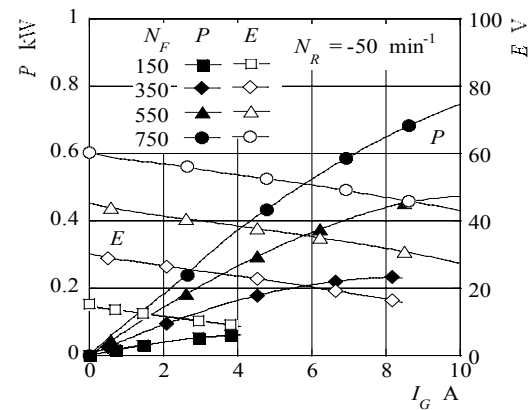


**Fig. 6** Output and the induced voltage against the induced electric current

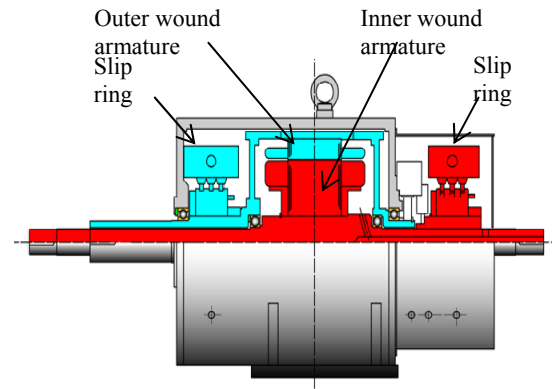


**Fig. 7** Model double rotational type doubly fed induction generator

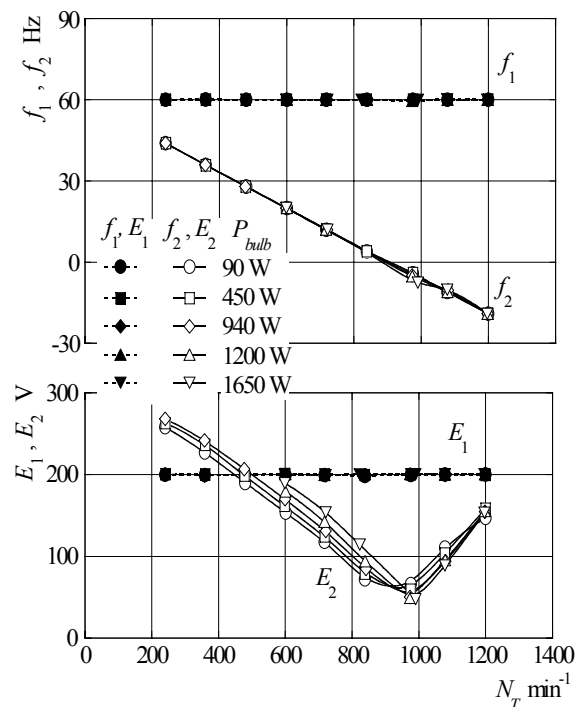


**Fig. 8** Frequencies and voltages against the relative rotational speed

of the inverter connected to the inner armature.

Figure 7 shows the trial model of the counter-rotating armature type doubly fed induction generator. The rated output is  $P = 1.2$  kW and the voltage is  $E_1 = 200$  V at  $N_T = 900$   $\text{min}^{-1}$ , where the number of the poles is 8. The characteristics were investigated as follows. The motor shaft was connected to the shaft of the inner armature while the shaft of the outer armature was kept stationary, because the electric characteristics depend only on the relative rotational speed between both armatures. The rotational speed of the motor, namely the rotational speed of the inner armature, which is the relative rotational speed, was controlled by the inverter. Another inverter controlled the frequency  $f_2$  and the voltage  $E_2$  which are supplied to the secondary feed (the inner armature) of the generator. The output was measured by the power meter and was consumed through the electric bulbs (the lamps,  $P_{bulb}$ ), while the frequency and the voltage induced from the outer armature (the primary feed) were kept constant at  $f_1 = 60\text{Hz}$  and  $E_1 = 200$  V.

Figure 8 shows the frequency  $f_2$  and the voltage  $E_2$  of the inner armature for keeping  $f_1$  and  $E_1$  of the outer armature constant, where  $N_T$  is the relative rotational speed ( $= N_F - N_R$ ,  $N_F$  and  $N_R$  are rotational speed of the inner and the outer armatures, and give the positive value in the  $N_F$  direction) as the same as the nomenclatures described above. The frequency  $f_2$  is in inverse proportion to the relative rotational speed  $N_T$  irrespective of the external load  $P_{bulb}$ , though the revolving direction of the magnetic field must be changed, which means that  $f_2$  is negative, at  $N_T$  faster than the synchronous speed  $900\text{min}^{-1}$ . The voltage  $E_2$  depends not only on  $N_T$  but also on  $P_{bulb}$ , namely the output  $P_1$ . The input  $P_2$  comes to be negative at  $N_T$  faster than  $900$   $\text{min}^{-1}$ , as shown in Fig. 9. That is,  $P_2$  changes fortunately from the input to the output, then the net output from the generator is  $P = P_1 - P_2$ .

## 2.4 Experimental Setup

The model hydroelectric unit shown in Fig. 1 was connected to the penstock and the discharge pipes in the test loop. The turbine head  $H$  and the discharge  $Q$  were given by the booster pumping system stood at the upstream, where  $Q$  was measured with the orifice and  $H$  was derived from the pressure on the casing walls at sections M1 and M4 in accordance with the standards/codes (IEC et al. [8]). Figure 10 proves the operation of the model unit with the above synchronous generator (Kanemoto et al [5]), where,  $N_{G11F}$  ( $= N_F D / H^{1/2}$  :  $\text{m, min}^{-1}$ ;  $D$ : the runner diameter = 245 mm) and  $N_{G11R}$  ( $= N_R D / H_G^{1/2}$  :  $\text{m, min}^{-1}$ ) are the unit rotational speed of the inner/front and the outer/rear armatures/runners,  $P_{G11}$  [ $= P_G / (D^2 H^{1/2})$  :  $\text{m, kW}$ ] is the unit electric output,  $M_{G11}$  [ $= M_G / (D^3 H)$  :  $\text{m, kN-m}$ ] is the unit rotational torque, and the runner blades were tentatively designed so as to get the axial flows at the inlet and the outlet of the tandem runners with  $N_F = -N_R$ . The rotational speeds  $N_{G11F}$  and  $N_{G11R}$  are adjusted themselves in response to the external bulb load, as the rotational torque  $M_{G11}$  of the inner armature coincides with that of the outer armature. The rotational speed  $N_{G11R}$  is in nearly proportion to  $N_{G11F}$ , and  $M_{G11}$  increases with the decrease of  $N_{G11F}$ . Such operations cause the increase of the

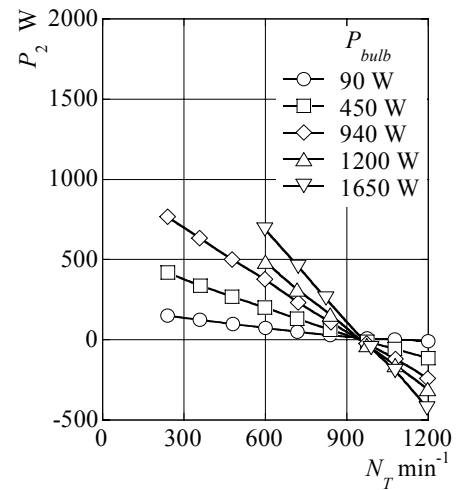


Fig. 9 Input against the relative rotational speed

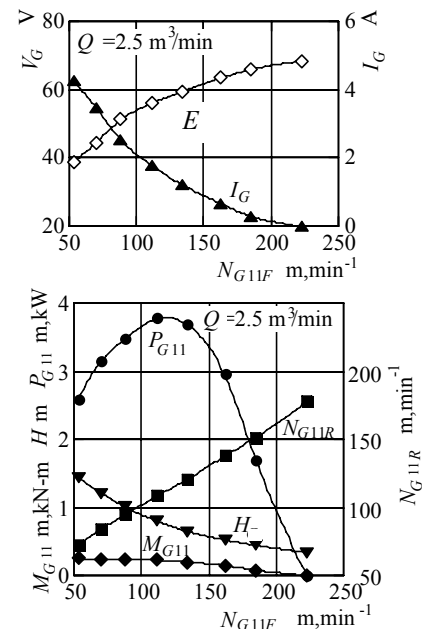


Fig. 10 Operation of the model unit

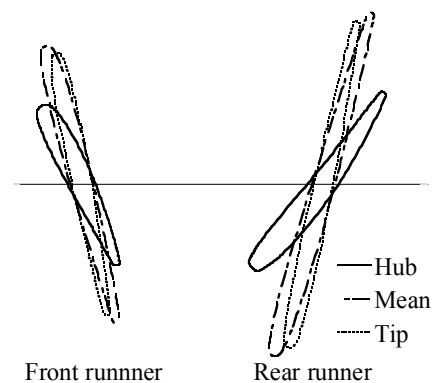


Fig. 11 Cross sections of Runner Blade C

turbine head  $H$  with the increase of the angular momentum change through the runners, namely  $M_{G11}$ , at the constant discharge. The induced electric current  $I_G$  goes down and the induced voltage  $E$  goes up with the increase of the rotational speed, and the runaway speed is about  $N_{G11F} = 225 \text{ m, min}^{-1}$ . The product  $3^{1/2} I_G E$  gives the electric output and  $P_{G11}$  is maximum with the induced frequency 27 Hz at  $N_{G11F} = N_{G11R} = 120 \text{ m, min}^{-1}$ .

In the followings, the front and the rear runner outputs were consumed with the regenerative braking circuit of the motor, respectively, in place of the peculiar generator shown in Fig. 1. The runner speeds were individually adjusted so that the rotational torque of the front runner coincides with that of the rear runner while the mechanical torque in the bearing and the pulley system was removed.

### 3. On-Cam Operation

#### 3.1 Preparation of Counter-Rotating Type Runners

To operate the counter-rotating type hydroelectric unit at the on-cam condition, the following runners were prepared. The diameter  $D$  is 245 mm, with the hub diameter of 90 mm and the casing diameter 250 mm. Figure 11 shows the runner blade sections, called here Runner Blade C, designed so as to take the flow conditions described in 2.1 and 2.4 at the normal operation. The camber lines of the front and rear blades are single arcs, and the thickness of both blades are referred to the NACA 0009 hydrofoils. In this paper, two types of runners were prepared using Runner Blade C, where Runner C23 is composed of two front blades and three rear blades and Runner C53 is composed of five front blades and three rear blades. Runner C23 may be suitable for the lower tidal head, namely the lower range of the tide, and Runner C53 may be suitable for the higher head, namely the higher range of the tide.

The model unit was operated at the relative rotational speed  $n_T = 900 \text{ min}^{-1}$  which corresponds to the frequency 60 Hz induced from the counter-rotating armature type generator with 8 poles. The setting angle of the blade was defined by the central angle around the twist center measured from the dimensions given in Fig. 11. These are shown by  $\theta_F$  for the front and  $\theta_R$  for the rear blades, where the angle is positive when the blade leans to the tangential direction (in the clockwise for the front blade, in the counter-clockwise for the rear blade in Fig. 11).

#### 3.2 Output and Hydraulic Efficiency

The variable discharge performances are shown in Fig. 12, where  $Q_{11}$  is the unit discharge  $[=Q/(D^2 H^{1/2})]$ : m, m<sup>3</sup>/s,  $P_{11}$  is the unit output  $[=P/(D^3 H^{3/2})]$ : m, kW,  $P$ : the shaft output defined by the standards/codes (IEC et al. [8]), and  $\eta_h$  is the hydraulic efficiency  $[=P/\rho g Q H]$ . The performances satisfy the similarity law for the traditional hydraulic turbines, and the experimental results are represented with the curves. The unit output  $P_{11}$  and the hydraulic efficiency  $\eta_h$  have the same features against the unit discharge  $Q_{11}$ , regardless of the blade setting angle and the number of the blade.

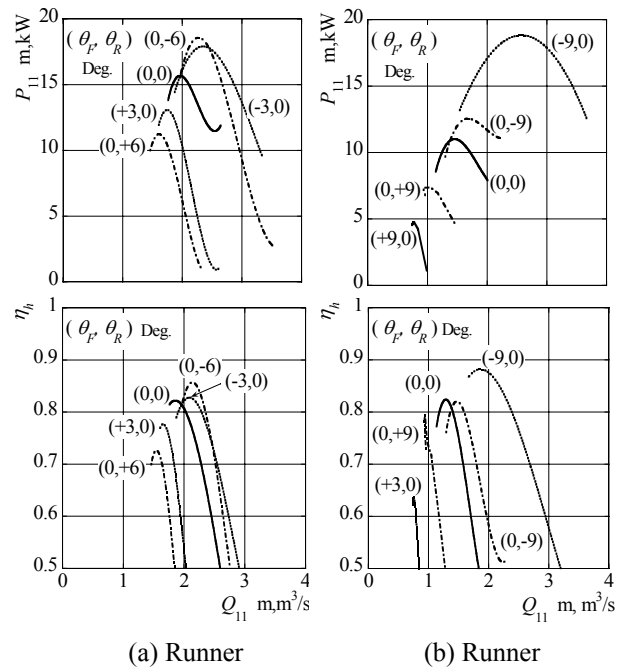
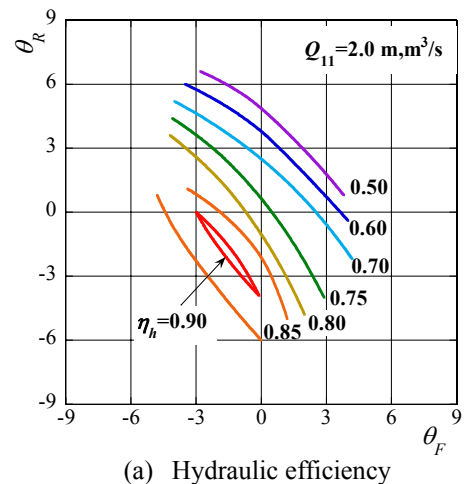
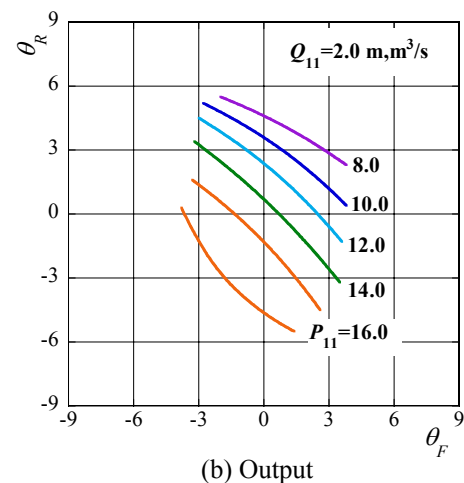


Fig. 12 Outputs and efficiencies of Runners



(a) Hydraulic efficiency



(b) Output

Fig. 14 Optimum blade setting angles at  $Q_{11} = 2 \text{ m, m}^3/\text{s}$  of Runner C23

The performances at the normal setting angle ( $\theta_F = \theta_R = 0$ ), however, suggest that Runner C23 is suitable for the higher discharge, namely the lower head, and Runner C53 is suitable for the lower discharge, namely the higher head, as expected at the design. The maximum output or the maximum efficiency is got at larger unit discharge with the decrease of not only the number of the blade but also the blade setting angle.

### 3.3 On-Cam Hill Chart

The relation between the unit relative rotational speed  $N_{11}$  [ $=n_T D/H^{1/2}$ : m, min<sup>-1</sup>] and the unit discharge  $Q_{11}$  for each blade setting angle ( $\theta_F, \theta_R$ ) are shown by the thin lines in Fig. 13, where these are derived from Fig. 12 and the hydraulic efficiency  $\eta_h$  and the unit output  $P_{11}$  on the each thin line were connected at the same value, and shown by the thick lines. That is, Fig. 13 gives the on-cam hill chart for the hydraulic efficiency  $\eta_h$  and the unit output  $P_{11}$ . This figure gives the optimum blade setting angle to operate the hydroelectric unit at the specified performances (Ida et al. [9]). To get the higher efficiency or output, the blades must be turned to the axial direction, as recognized in Fig. 14. At such blade adjustments, for instance, the maximum efficiency is at the lower discharge  $Q_{11}$  and at the lower rotational speed  $N_{11}$ .

## 4. Operation at Bidirectional Flows

### 4.1 Modification of Blade Profiles

As mentioned above, it is necessary to set uselessly/unfortunately a pair of the traditional type hydroelectric

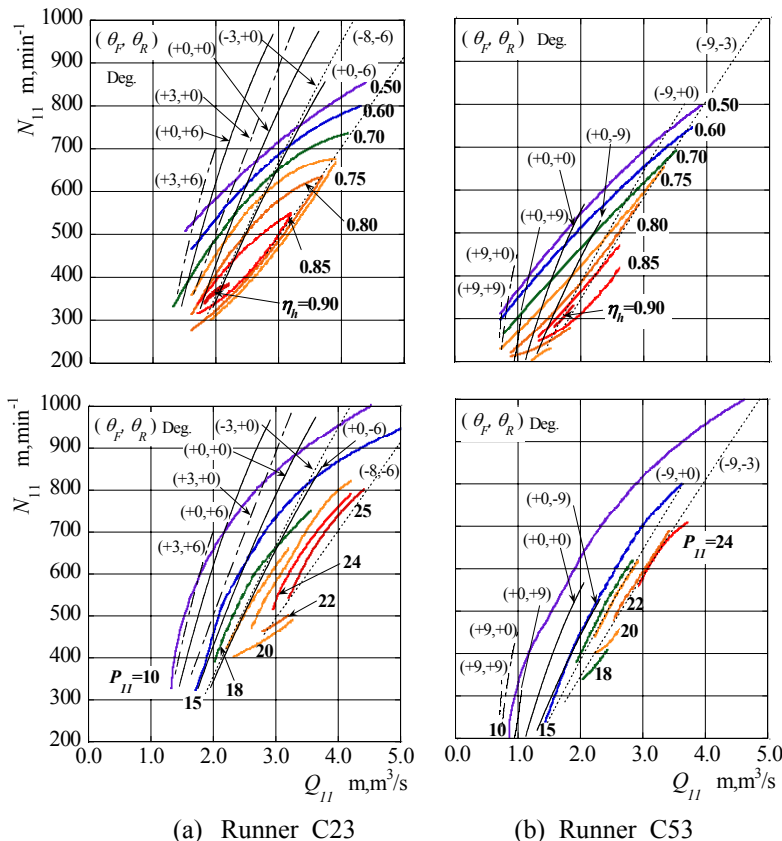


Fig. 13 On-cam hill charts

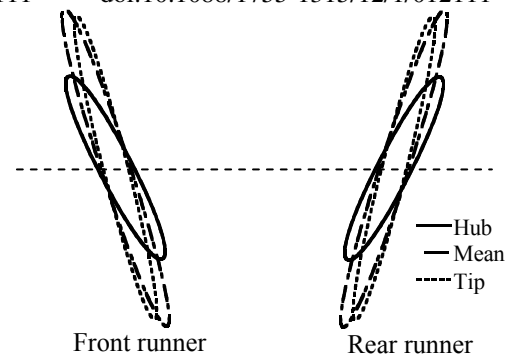


Fig. 15 Cross sections of Runner Blade D

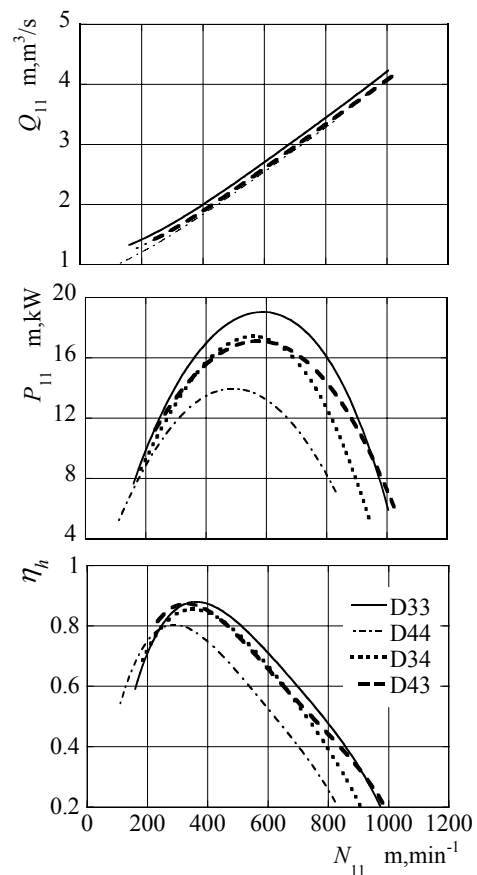


Fig. 16 Performances of Runner D

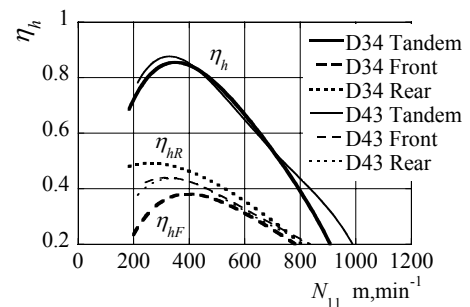


Fig. 17 Hydraulic efficiency of Runner D34 and D43



units whose nose and tail are replaced each other, for utilizing sufficiently the rising and the falling tidal energies. The counter-rotating type hydroelectric unit is, however, effective to both flow directions because the flow discharged from the rear runner is in the axial direction while the swirl-less flow attacks to the front runner as expounded above. Such flow conditions suggest that the counter-rotating runners can be supplied to both rising and falling tidal flows at the power station.

Then, the runner blades were modified so as to work effectively at the both flow directions, as shown in Fig. 15 (Runner Blade D), where the head  $H = 1.75$  m and the discharge  $Q = 0.28$  m<sup>3</sup>/s at the relative rotational speed  $N_T = 1,500$  min<sup>-1</sup>. The blades have the symmetrical hydrofoils without the camber. The trailing edge is also the same profiles as the leading edge, and the rear blade is the same profiles as the front blade. The diameter of the runners is 245 mm with the hub diameter of 90 mm and the casing diameter 250 mm, as the same as the blades shown in Fig. 11.

To know the turbine performances and the flow conditions, four type runners called Runner D33, D34, D43 and D44 were prepared, where D gives the runner profiles, the numerical values give the front and rear blade numbers in order, and the runner blades were set at the hub shown in Fig. 1. In the experiments, the runner speeds were not adjusted so as to keep the induced frequency constant, but the rotational torque was undoubtedly adjusted between both armatures/runners.

## 4.2 Turbine Performances

The variable head characteristics, that are the performances against the unit relative rotational speed  $N_{11}$ , are investigated experimentally and shown with the curves in Fig. 16. The performances against  $N_{11}$  have almost the same features and the maximum outputs are at  $N_{11} = 500$ -600 m, min<sup>-1</sup>, regardless of the runner profiles. Judging from the relative rotational speed giving the maximum output, among the runners prepared in this paper, Runner D33 is suitable for the higher discharge  $Q_{11}$  at the higher  $N_{11}$ , namely the lower head, and Runner D44 is suitable for the lower  $Q_{11}$  at the lower  $N_{11}$ , namely the higher head.

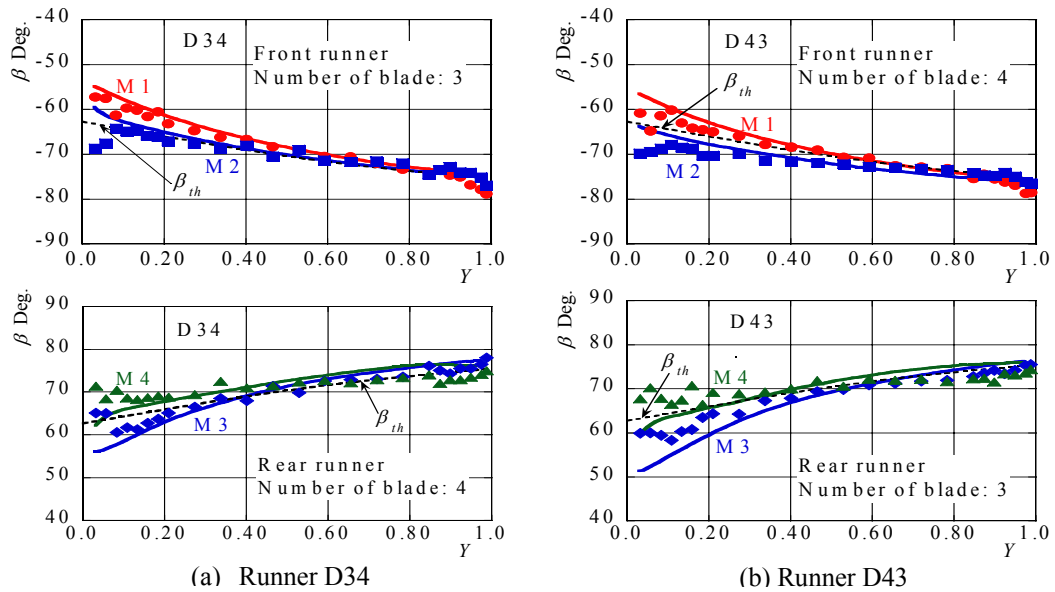
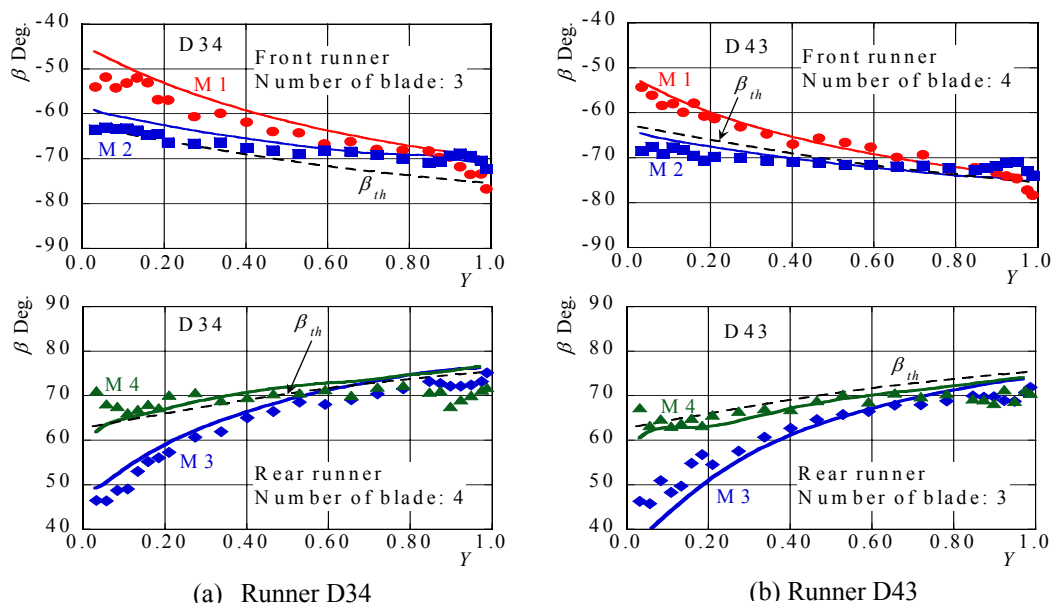
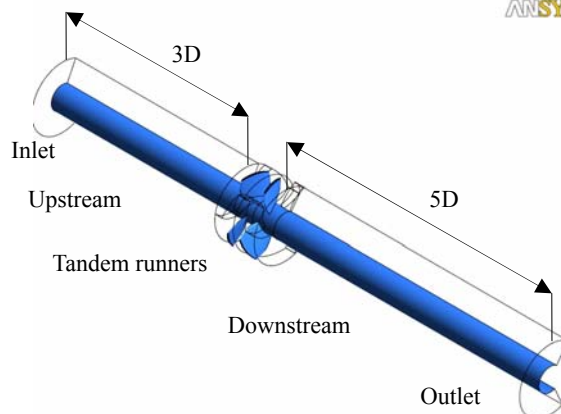
The maximum hydraulic efficiencies are at  $N_{11} = 250$ -350 m, min<sup>-1</sup>, and the values are almost the same those at the higher  $Q_{11}$  in Fig. 12. Figure 17 shows the hydraulic efficiencies of Runners D34 and D43, where D43 means that the flow direction is changed from the direction for D34. The efficiency of the front runner  $\eta_{hF}$  with 4 blades (Runner D43: the thin dash line) is higher than that with 3 blades (Runner D34: the thick dash line), and the efficiency of the rear runner  $\eta_{hR}$  with 4 blades (Runner D34: the thick dash line) is higher than that with 3 blades (Runner D43: the thin dash line). Resultantly, the flow direction hardly affects the hydraulic efficiency  $\eta_h$  of the reversible/bidirectional type runners even if the front and the rear blade numbers are reasonably changed (see  $\eta_h$  drawn by the full lines in Fig. 17). These efficiencies are almost the same as  $\eta_h$  of Runner D33 (the thin full line in Fig. 16), but are obviously higher than  $\eta_h$  of Runner D44 (the thin dot-and-dash line in Fig. 16).

## 4.3 Flow Conditions around Runners

Flow conditions around the at the maximum output and the maximum hydraulic efficiency are shown in Figs. 18 and 19, where  $\beta$  is the relative flow angle measured from the axial direction (see Fig. 2) and averaged in the tangential direction,  $Y$  is the dimensionless distance measured from the hub to the casing walls,  $\beta_{th}$  drawn by the thin dash line is the blade setting angle without the camber. The relative flow angles discharged from the runners are close to  $\beta_{th}$  at the maximum output (Fig. 18) where the runners were designed, but the flows deviate slightly from  $\beta_{th}$  at the maximum hydraulic efficiency (Fig. 19). The runner has to get the angular momentum change from the through flow, even if the blade has no camber. The relative flow has the positive attack angle at the leading edge and is discharged from the trailing edge along the blade camber. That is, the momentum change always accompanies with the shock loss at the leading edge but the loss is tiny, because the flow along the suction surface of the blade does not separate in the following flow simulation even operating at the maximum efficiency with the large attack angles.

To prepare the design tool for optimizing the runner profiles, the flow conditions around the runners were simulated numerically with the commercial code ANSYS CFX-11, where the region of the simulation is shown in Fig. 20. The region from the inlet to the outlet sections was divided into the upstream (node number: 123,000), the front runner (node number: 266,000), the rear runner (node number: 352,000) and the downstream (node number: 155,000) sub-regions, and each sub-region was connected with the frozen-rotor interface. The relative flow angles are shown by the thick full lines in Figs. 18 and 19, and it is confirmed that the flow conditions are predicted well with the commercial code. The code may be useful to design the runners at the future steps.



**Fig. 18** Relative flow angles at the maximum output**Fig. 19** Relative flow angles at the maximum efficiency**Fig. 20** Flow region in the numerical simulation

## 5. Concluding Remarks

The counter-rotating type hydroelectric unit was operated at the on-cam condition. The runners with small number of the blade are suitable for the higher discharge, namely the lower head. The maximum output or the maximum efficiency is got at the higher unit discharge with the decrease of the blade number. The on-cam hill chart against the unit discharge or the unit relative rotational speed was also presented. This chart gives the optimum blade setting angles to operate the unit at the specified efficiency or output. To get the higher efficiency or the higher output, the blades must be turned to the axial direction. At such blade adjustments, the maximum efficiency is at the lower discharge or at the lower rotational speed, and the maximum output is at the higher discharge or at the higher rotational speed.

At the tidal power station with the traditional type hydroelectric unit, a pair of the units, whose nose and tail are replaced each other, must be set unfortunately/ uselessly, to get the fruitful output from not only the rising but also the falling tide. The tandem runners in the counter-rotating type hydroelectric unit are, however, effective to both flow directions because the flow is discharged from the rear runner in the axial direction while the swirl-less flow attacks to the front runner. Then, the runner blades were modified so as to work sufficiently at both rising and falling tidal flows, and the hydraulic performances were investigated experimentally. The performances against the unit relative rotational speed have almost the same features as those of the normal runners which are designed so as to be suitable for one way flow. The unit discharge giving the maximum output is higher than one giving the maximum efficiency irrespective of the blade number, and the efficiencies are almost the same as those of the normal runners. The relative flow has the positive attack angle at the leading edge and is discharged from the trailing edge along the blade camber. That is, the momentum change always accompanies with the shock loss at the leading edge. Such flow conditions were also predicted numerically by the commercial CFD code.

## Acknowledgments

The authors wish to thank Mr. Makoto Usui and Mr. Tetsuro Kasai who were graduated from Kyushu Institute of Technology (KIT) in Japan, and Mr. Yoshihiro Nakamura who is student of Graduate School of Engineering, KIT, for helping the experiments. Some parts of this research were in collaboration with Professors Toshiaki Setoguchi and Shuichi Nagata from Institute of Ocean Energy, Saga University.

## References

- [1] [http://www.dpa.unina.it/adag/eng/renewable\\_energy.html](http://www.dpa.unina.it/adag/eng/renewable_energy.html), <http://www.marineturbines.com/home.htm>.
- [2] Furukawa A, Gajanayake P A and Okuma K 1998 Application of Darrieus-Type Turbine Developed for Low Head Hydro-Power to Tidal Power Generation System, *Proc. of the 8th Int. Offshore and Polar Engin. Conf. 1998* vol 1 (Montreal, Canada) pp 155-61
- [3] Fukutomi J and Nakase Y 1997 Cross-Flow Turbine with Axis-symmetric Casing for Wave Power Conversion *Proc. of the 5th Asian Int. Conf. on Fluid Machinery 1997* vol 3 (Seoul, Korea) pp 849-56
- [4] Nielsen T K, Royrvik J, Ramdai J and Dahlhaug O G 2006 Propeller Turbine with Two Contra-Rotating Impellers and Built in Generator *Proc. 23rd IAHR Sym.*F146.pdf. (Yokohama, Japan)
- [5] Kanemoto T et al. 2000 Counter-Rotating Type Machine Suitable for Tidal Current Power Generation *Proc. of the 10th Offshore and Polar Eng. Conf.* vol 1 pp 472-477; Kanemoto T et al. 2001 Tidal Current Power Generation System for Boarding on a Floating Buoy *Int. J. of Offshore and Polar Engineering* **11**(1) 77-79; Kanemoto T 2001 Counter-Rotating Type Machine Suitable for Micro-power Generation *JETRO New Technology in Japan* **29**(1) 6
- [6] Tanaka D and Kanemoto T 2006 Experimental Study on Design Materials for Solidity of Counter-Rotating Runners *Proc. of the 23th IAHR Symp.*F147. pdf. (Yokohama, Japan)
- [7] Muller S, Deicke M and De Doncker RW 2000 Adjustable Speed Generator for Wind Turbines based on Doubly-fed Induction Machines and 4-Quadrant IGBT Converter Linked to the Rotor *Conf. Record of the 2000 IEEE* vol 4 pp 2249-54
- [8] IEC 1989 *IEC-TC4 (C0) 48*; Japanese Electric Association 1991 *JEC-4001&4002*; The Japan Society of Mechanical Engineers 1999 *JSME S008*
- [9] Ida I et al. 1991 Hydroturbine *Turbomachinery Society of Japan* 58-89